water

MDPI

Article

The Method for Evaluating Cross-Shore Migration of Sand Bar under the Influence of Nonlinear Waves Transformation

Margarita Shtremel [1,*], Yana Saprykina [1] and Berna Ayat [2]

[1] Shirshov Institute of Oceanology, Russian Academy of Sciences, 117997 Moscow, Russia; saprykina@ocean.ru
[2] Department of Civil Engineering, Yildiz Technical University, Istanbul 343420, Turkey; bayat@yildiz.edu.tr
* Correspondence: shtremel@ocean.ru

Abstract: Sand bar migration on the gently sloping sandy bottom in the coastal zone as a result of nonlinear wave transformation and corresponding sediment transport is discussed. Wave transformation on the intermediate depth causes periodic exchange of energy in space between the first and the second wave harmonics, accompanied by changes in the wave profile asymmetry. This leads to the occurrence of periodical fluctuations in the wave-induced sediment transport. It is shown that the position of the second nonlinear wave harmonic maximum determines location of the divergence point of sediment transport on the inclined bottom profile, where it changes direction from the onshore to the offshore. Such sediment transport pattern leads to formation of an underwater sand bar. A method is proposed to predict the position of the bar on an underwater slope after a storm based on calculation of the position of the maximum amplitude of the second nonlinear harmonic. The method is validated on the base of field measurements and ERA 5 reanalysis wave data.

Keywords: nonlinear wave transformation; coastal zone; sand bars; cross-shore sediment transport

Citation: Shtremel, M.; Saprykina, Y.; Ayat, B. The Method for Evaluating Cross-Shore Migration of Sand Bar under the Influence of Nonlinear Waves Transformation. *Water* **2022**, *14*, 214. https://doi.org/10.3390/w14020214

Academic Editor: Federica Rizzetto

Received: 10 November 2021
Accepted: 9 January 2022
Published: 12 January 2022

1. Introduction

Sand bars as morphological forms are found almost everywhere on the gentle coastal slopes of the seas and oceans. Their formation and behavior are the result of the interaction of waves and currents, and their dynamics can largely characterize the state of the coastal zone [1,2]. Underwater sand bars can act as a natural protection of the beach from wave impact as the waves break and lose their energy when passing over them due to the shallower depth above the top of the bar. During strong storms, sand bars reduce coastal run-up and inundation which can lead to erosion of dunes and cliffs [3]. The dynamics of sand bars determines the morphological variability of the coastal zone.

During storms, high waves break on the top of bars and cause strong offshore currents ("undertow") that transport the sediment toward the sea, resulting in sand bar migration from the coast and beach erosion [4]. During the attenuation of the storm and decreasing in the heights and periods of the waves, as well as at moderate energy wave conditions, the sediment transport due to wave nonlinearity leads to a gradual migration of sand deposits, accompanied by accumulative processes of beach restoration (for example, [4,5]). In addition to movement on the time scale of individual storms, it has been noted by many researchers that sand bars migrate quasi-periodically depending on the seasonal wave climate during the year [6,7]. Cyclic bar movements were also observed on a scale of several years or decades, which is associated with global changes in the wave climate, depending on the main teleconnection patterns [6,8], but sometimes the behavior of the sand bar at a scale of several years does not depend only on the wave action, but also on tides and currents, such as the long-term migration of the bars from the coast to offshore noted in [9]. Influence of wave actions is very complex. In the long term period, the largest wave events are responsible for bar location which then changes due to seasonal (winter/summer) variations in wave height. Additionally, the order of several storms can have an effect on bar shape and lead to episodic bar migration [9].

In general, based on the conclusions of numerous modern research, the movement of sand bars in the coastal zone still remains a challenge for researchers and there is no single concept or universal model of the detailed physical mechanisms describing their movement at all time scales [10].

Meanwhile, the knowledge of the patterns of bar movement is important for coastal engineering in order to construct coastal infrastructure or protection, as well as for the development of a strategy aimed at using a beach for recreational purposes. For example, the position of the underwater sand bar relative to the coastline can have both coastal protection and erosion effects [11] and the formation of a bar as a morphological structure can lead to shore erosion, but its movement and, ultimately, its merging with berm, can induce the accumulation of sand on the coast. Such processes can be cyclical with a period from days to several years.

Several models have been developed to simulate the behavior of sand bars at different time scales from several days to years: models based on the wave breaking point concept, which calculate the migration of a sand bar from an equilibrium position depending on wave height [12], data-driven models based on neural networks [13], and averaged process-based models [9,14–17].

However, a number of limitations remain for these models. For example, some of them successfully describe the motion of existing bars, but do not describe the process of their formation. Another limitation is mainly related to the fact that the nonlinear processes of wave transformation and the associated nonlinear changes in the asymmetry and skewness of bottom velocities and accelerations affecting sediment transport are not sufficiently taken into account. The contribution of nonlinearity is usually implemented through empirical dependencies that are obtained for laboratory conditions or for conditions of a specific coastal zone and are not generally universal. For example, such a relationship based on the Ursell number is used in the widely used Xbeach model [14,18]. The models are often very complex and time-consuming, which limits their application for operational coastal management. Therefore, for a qualitative express assessment of the movement of sand bars, for example on the short time scale of one or several successive storms or seasonal cycle storms for coastal zone management, or for the geographical description of a coastal zone, more simple methods are needed.

The purpose of this work is the development and validation of a simple method for estimating the position of a sand bar based on the nonlinear properties of wave transformation over a given bottom slope.

2. Data

2.1. Study Site and Morphological Survey Data

The study site is located on the open coast of the Vistula spit (Figure 1) near the city of Baltiysk. The spit in this region is oriented from SSW to NNE with 32 degrees azimuth. The coastal zone of the polygon is characterized by a 30–35 m wide beach adjacent to the mild (bottom slope tangent is equal to 0.01) sandy bottom slope with two sand bar systems. Sand bars are very dynamic, moving seaward and shoreward, changing shape from crescentic to near parallel to the coast over time, possibly dependent on dominant wave direction. The coastline also changes its form, varying from cuspate to straight.

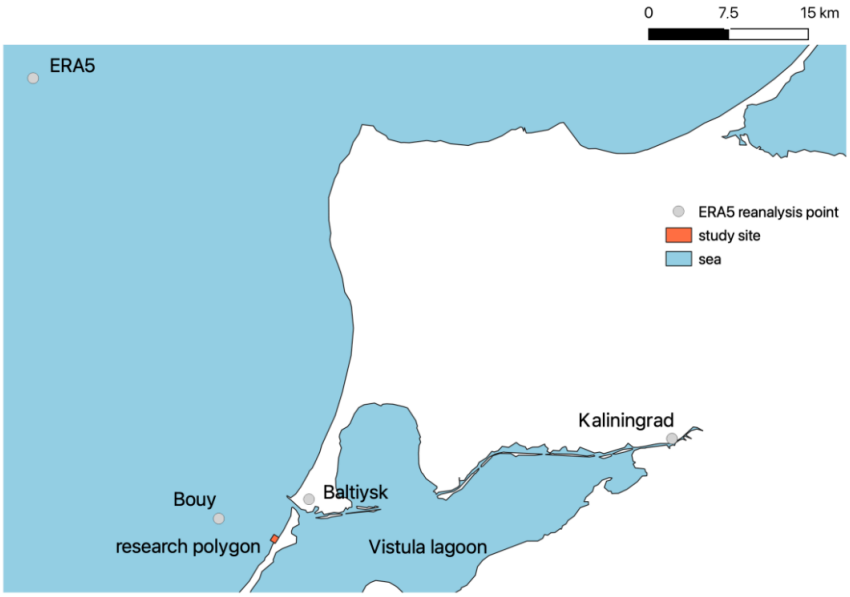

Figure 1. Study site, region of the bathymetry measurements (small pink rectangle), ERA5 point and buoy location.

Regular measurements of coastal bathymetry on the study site (Figure 1) started in May 2019. In total 4 measurements were carried out: in May and November 2019, and March and November 2020. The size of the measured area was 600 × 500 m. The depth measurements were carried out from a small vessel with the Garmin GPS Map 580 Plus echo sounder. Twenty shore-normal tacks with 30 m distance between them were made. Depth values were recorded each second, which gives around 1–1.5 m spatial resolution. Depth accuracy for such measurements is 10 cm.

The bathymetry data obtained with an echo sounder mounted on the boat transom is limited to 0.5–0.8 m depth. Shallower regions are not covered, so satellite data were used to detect the coastline position. As shown in Figure 2, coastal forms such as the sand bar crest positions determined from the field measurements correspond to those detected from satellite images. Therefore, it is possible to use satellite data for the nearshore relief study.

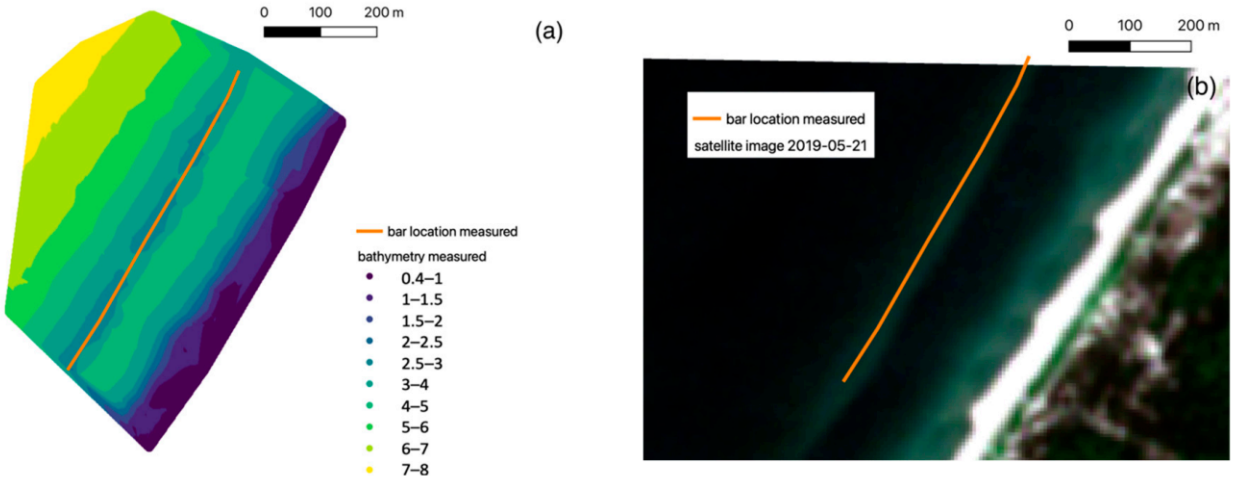

Figure 2. Sand bar crest position detected (**a**) with field measurement (23 May 2019) data (**b**) in the satellite image (Sentinel-2) captured on 21 May 2019.

To obtain the coastline position the optical data of Sentinel-2 with 10 m resolution was used. There are two satellites in this mission that give an image of the studied region around every two days. Images with the clearest view of the coastline and closest to the date of the bottom topography measurements were chosen. These were 21 May and 17 November in 2019, and 26 March and 1 November in 2020. Shoreline detection was carried out visually (Figure 3).

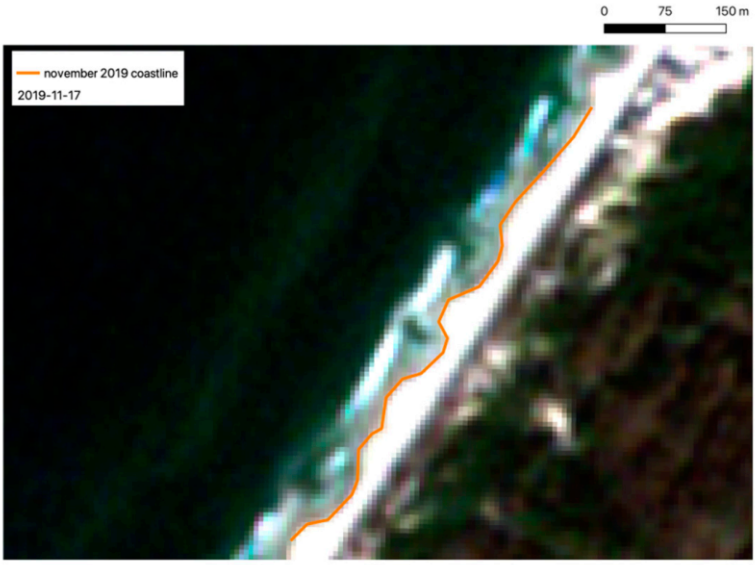

Figure 3. Example of visual shoreline detection based on satellite image.

The studied part of the Vistula spit coastal zone demonstrates cyclic morpho-dynamic behavior when the sand bar initially forms offshore in deep water and then migrates onshore, merging with the coast.

During the 1.5 years of relief measurements, part of such a cycle was captured starting with a newly-formed shore-parallel sand bar in May 2019 along with its subsequent shoreward migration (Table 1) and ending with its near merging to the beach in November 2020 (Figure 4).

Table 1. Distance from the shoreline to the sand bar crest (location of the sand bar) and incline of the seaward bottom slope of the sand bar.

Date of Measurements	Sand Bar Offshore Distance, m	Bottom Slope
23 May 2019	210–220	0.0185
8 November 2019	200	0.0169
23 March 2020	170–190	0.0161
13 November 2020	130–180	0.0136

These processes are accompanied by changes of the bottom slope seaward of the outer sand bar from 0.0185 in May 2019 to 0.0136 in November 2020 (Table 1). The value of this slope affects wave transformation processes, as will be shown below.

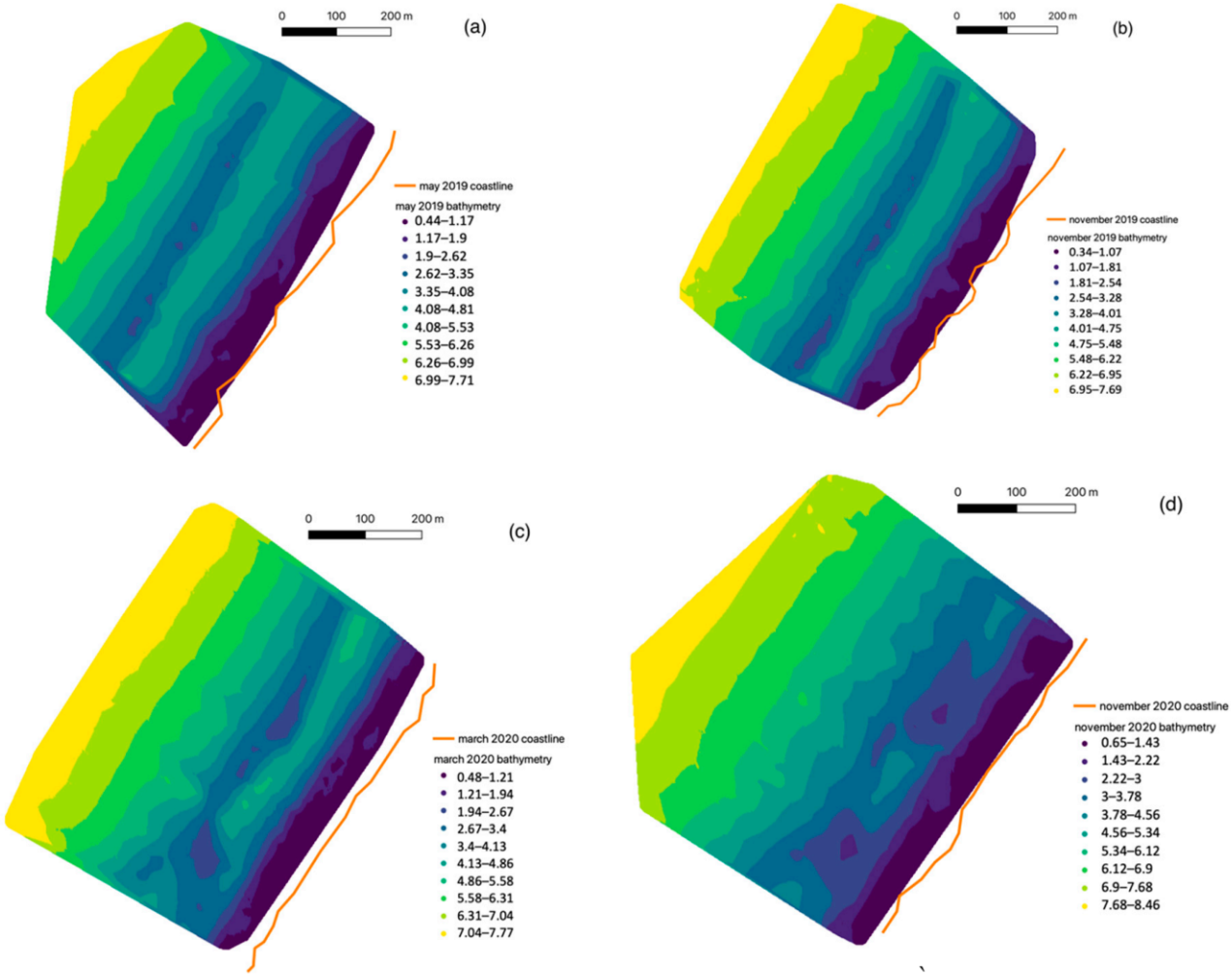

Figure 4. Bathymetry maps obtained during expeditions in 2019–2020. (**a**) 23 May 2019, (**b**) 8 November 2019, (**c**) 23 March 2020, (**d**) 13 November 2020.

2.2. Wave Data

As a source of wave data ERA5 reanalysis was used. This has a 1 h timestep and 0.5-degree spatial resolution [19]. To assess the accuracy of the reanalysis data for real waves in a given region, we compared them with data from the buoy for July 2019 [20]. Wave measurements with the Spotter buoy used for the ERA5 reanalysis wave data validation were carried out on 11–27 July 2019, at 20 m depth, 5.3 km distance from the Vistula Spit, Kaliningrad Region of Russia, Baltic Sea coast (54.63° N 19.77° E, Figure 1). Despite the fact that the nearest point to the buoy and to the study site had coordinates 54.5° N 19.5° E, the best correspondence was found at the point with 55° N 19.5° E coordinates which was located farther offshore (Figure 1).

A number of reanalysis wave parameters are available, such as peak and mean wave period, wave height, peak and mean direction both of combined swell and wind waves and of swell and wind waves separately. In this study we analyze combined parameters of wind waves and swell: peak direction, significant wave height and peak period.

3. Results: Sand Bar Migration Assessment Method

3.1. Calculation of Second Wave Harmonic Maximum Position

The influence of nonlinear transformation of waves and a spatially periodic change in their symmetry on the formation of underwater bars were first noted in [21]. According to field observations for the Georgian Bay of Lake Ontario and modelling on the base of

monochromatic waves, the formation of underwater bars depended on the position of the maximum of the second harmonic amplitude. Later this assumption was also confirmed by the data of a field experiment in the Black Sea [5].

A quasi-periodic change in wave symmetry during nonlinear wave transformation occurs due to near resonant triad wave interactions and interference of free and bound waves [22]. For spatial evolution of frequency wave spectra, this manifests as a periodic exchange of energy between the amplitudes of the first and second wave.

During one period of energy exchange between first and second harmonics throughout the beat length, the amplitude of second nonlinear harmonic grows to its maximum and then decreases again. Four main scenarios of nonlinear transformation of waves with periodical energy exchange were identified in [23].

The scenarios differ in the number of possible observed beat lengths and the magnitude of the second harmonic amplitude. The implementation of any scenario for a given bottom slope depends on the relationship between the wave steepness (H/L, where H is deep water wave height, and L is deep water wavelength) and the Iribarren number (or coastal zone similarity parameter):

$$\mathrm{Ir} = \frac{\tan\alpha}{\sqrt{\mathrm{H/L}}}, \tag{1}$$

where $\tan\alpha$ is the bottom slope value.

As shown in [6], the movement of the sand bar to the coast and from the coast occurs in the scenario of wave transformation with one clearly pronounced spatial period exchange of energy between harmonics and with one absolute maximum of the second harmonic amplitude. The criterion for such a scenario is as follows:

$$\mathrm{Ir} < 7\mathrm{H/L} \tag{2}$$

The dependence of underwater sand bar movement off and on shore on the incoming waves' steepness was also observed in a laboratory experiment [24]. Thus, we can assume that for a given bottom slope, the wave steepness is a parameter which determines the scenario of nonlinear wave transformation, the position of the second harmonic amplitude maximum and the position of the underwater bar top [5,6,21].

As shown in [5], the position of the second harmonic maximum sets the divergence point on the bottom profile, relative to which the bottom topography deformations occurin different directions, which leads to the formation of an underwater bar. The main reason is the deterministic change in the phase shift (bi-phase) between first and second nonlinear wave harmonics, which directly influences the change in the waves and bottom velocities' symmetry. The bi-phase varies in the range $(-\pi/2, \pi/2)$ and zero value corresponds to the maximum amplitude of the second harmonic [5,25]. When the wave conditions and the scenario of nonlinear transformation change, the position of the divergence point (or the position of the maximum of the second harmonic amplitude) will change also and, accordingly, the sand bar will move. Thus, for a qualitative assessment of the bar motion, it is necessary: (a) to assess the presence of the corresponding scenario of nonlinear transformation of waves and (b) to calculate the position of the second harmonic amplitude.

If parameters of incoming waves (height, period or wave steepness) and mean bottom slope are known, the type of wave transformation scenario can be defined by criterion (2).

So, step 1 of the proposed methodology is to determine whether the scenario that leads to sandbar migration will occur using criterion (2).

Step 2 is to define the location of the second wave harmonic maximum. According to [23], in which the empirical dependence for bi-phase on beat length was suggested, the nearest maximum of second harmonic where bi-phase equals zero will be located 1.5 beat lengths off the shoreline. Thus, having calculated the beat length, we can obtain the locus of the points corresponding to the positions of the second harmonic (a_2) maximum.

The spatial period of wave energy exchange or beat length (L_b) can be calculated by the following Equations [22]:

$$L_b = \frac{2\pi}{\delta_k} \tag{3}$$

$$\delta_k = 2k_1 - k_2 \tag{4}$$

where k_1, k_2 are the first and second harmonic wavenumbers, which can be calculated, for example, using linear dispersion relation:

$$\omega^2 = gktanhkh \tag{5}$$

where ω is angular frequency, g is gravitational acceleration, and h is depth.

The position of the second harmonic maximum can be calculated by the iterative method based on Equations (3)–(5). Starting with the depth where wave parameters are available, wavenumber mismatch δ_k and corresponding beat length L_b are calculated using linear dispersion relation (Equations (5)), then depth of the nearest to the shore maximum as the depth at 1.5 L_b distance from the shoreline is evaluated. Then it is substituted in the mismatch calculation equation, instead of the starting depth value. The process is repeated until the difference in the predicted L_b value between iterations becomes small enough (i.e., 5% of the L_b value, or the criterion to stop the iterative process chosen by the researcher).

3.2. Analysis of the Wave Parameter Series

Step 3 of the proposed methodology is to assess the wave parameter time series. As the initial data, significant wave height, peak wave period and direction are used.

Wave transformation processes mainly affect bottom slope relief and bar movement during the action of the shore–normal waves. Therefore, we will consider for the assessment of bar position shore normal directed waves only, which gives us step 3a: separate shore-normal waves regimes from the res-. Waves are assumed shore-normal if they approach the shoreline with $90 \pm 45°$ angle.

Step 3b is to determine which wave regimes play the major role in the sand bar migration processes. The following metric M (Equation (6)) is suggested. First, all the wave regimes were grouped into 20 bins of the bivariate histogram depending on the value of the second harmonic maximum distance off the shoreline (Da_2) and significant wave height. A histogram is a way to analyze the time series of the wave regimes and to reveal those that affect sand bar migration the most. It shows joint distribution of Hs and distance of the second harmonic maximum location off the shoreline. As the wave characteristics in the reanalysis are available at a 1 h timestep, the number of values that fall in each bin indicates the time of the action of waves with the parameters that lay in the specific bin's range during the considered period (in our case the period between relief measurements). In this way, the histogram allows determination of where the second harmonic maximum is most often located. Wave height (H) value indicates whether the waves will influence the relief to a greater or lesser degree, as the most repetitive regimes are usually characterized by small wave heights and will not affect the relief as much as higher waves that are not so common. The size of the bins is chosen empirically to be small enough to represent the spatial structure of the wave regime's distribution (20 bins gives around 5 m spatial resolution) and wave height step 0.2 m. Smaller resolution (more bins with smaller ranges of the considered parameters) will be hard to interpret due to the small number of regimes that will fall into each bin. If, on the other hand, the coarser division is used, the tendencies will be the same, but as the center values of each bin are analyzed, the positions of the most persistent second harmonic maximum locations can be biased.

Then the number of counts in each bin was weighted by the dimensionless relation between the wave height and depth of the a2 maximum. Such weighting allows assessment of which regimes affect underwater bathymetry the most, as the higher the waves in the smaller water depth, the more significant impact they have on the bottom slope deformation.

Then all the values of the weighted number of counts corresponding to the specific a2 distance were summed and related to the total sum.

$$M = \frac{\left(\sum_i n_{i,j} \frac{H_i}{d_j}\right)}{\left(\sum_{i,j} n_{i,j} \frac{H_j}{d_j}\right)} 100 \quad (6)$$

where $n_{i,j}$ is the number of counts in the i, j-th bin, H_i is the wave height corresponding to the center of the *i*-th bin, and d_j is the depth of the second harmonic corresponding to the *j*-th bin center.

The maximum of such metric indicates the position of the second harmonic maximum distance from the shoreline which affects the underwater bottom and sand bar migration the most. The new sand bar position is expected to move between this point (1.5 L_b offshore) and the point with the second harmonic minimum (1 L_b offshore).

4. Discussion of Results

For the validation of the suggested method the wave data will be divided into three time intervals according to the time between bottom relief surveys to predict sand bar position and compare this with observations.

4.1. Time Period 1: 24 May–8 November 2019

Due to the outer sand bar formation prior to the start of the observations at the study site, seaward slope of the bar reached 0.0185. With such a bottom slope value during the considered time period, wave regimes with periodic exchange of energy between harmonics made up only 57% of all regimes (Figure 5).

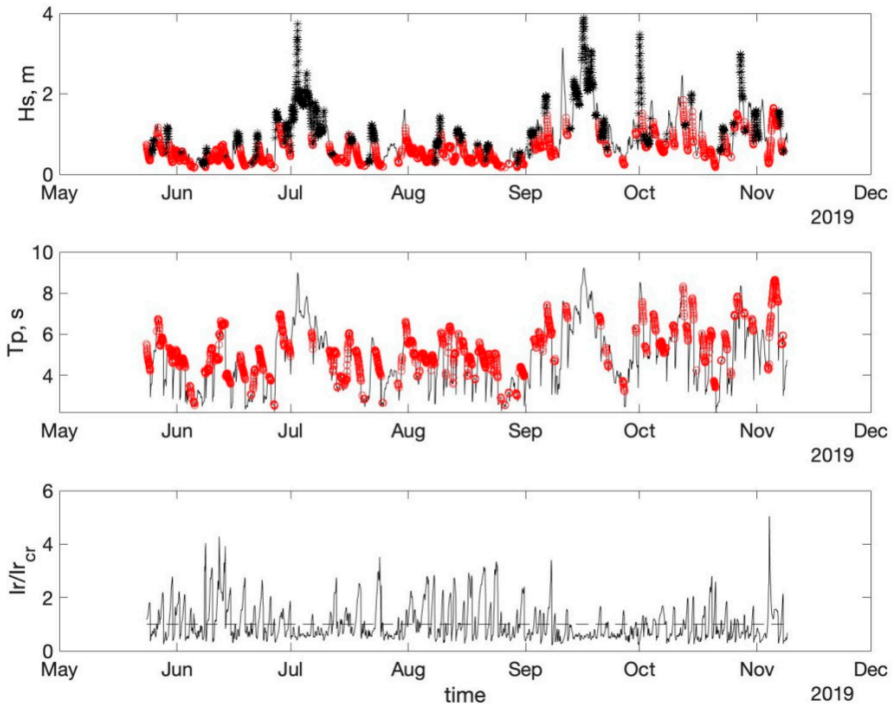

Figure 5. Wave height, peak wave period and ratio between deep water and critical Iribarren number (below the dashed line are regimes with pronounced exchange of energy between wave harmonics). Red circles—wave regimes without pronounced energy exchange between harmonics. Black stars—shore-normal regimes.

Red dots in the lower plot in Figure 5 show critical values of the Iribarren number that divide scenarios with pronounced periodical exchange of energy between harmonics and

those where second harmonic values are small within the coastal zone (Equation (5)). The latter are shown with red circles in the two upper plots in Figure 5.

As can be observed in Figure 5, the highest waves during the storms lead to scenarios of wave transformation with one pronounced periodic exchange of energy between harmonics.

All the wave directions were divided into 2 parts: shore-normal and oblique. Waves that approach from the 272–332 rhumb are considered shore-normal. As shown in Figure 5, waves with shore-normal approach include about 1/3 of all wave regimes.

The maximum of the parameter M (Equation (6)) corresponds to the regimes with D_{a2} located 100 and 170 m off the shoreline. The sand bar moved onshore only slightly (about 10 m) (Figure 4). This may be due to the fact that the second harmonic maximum point and the corresponding divergence point were located far more shoreward with respect to the sand bar crest location for most of the time (Figure 6). The wave regimes with second harmonic maximum position at 250 m distance off the shoreline (seaward of the sand bar crest) have wave steepness in the range of [0.026, 0.03].

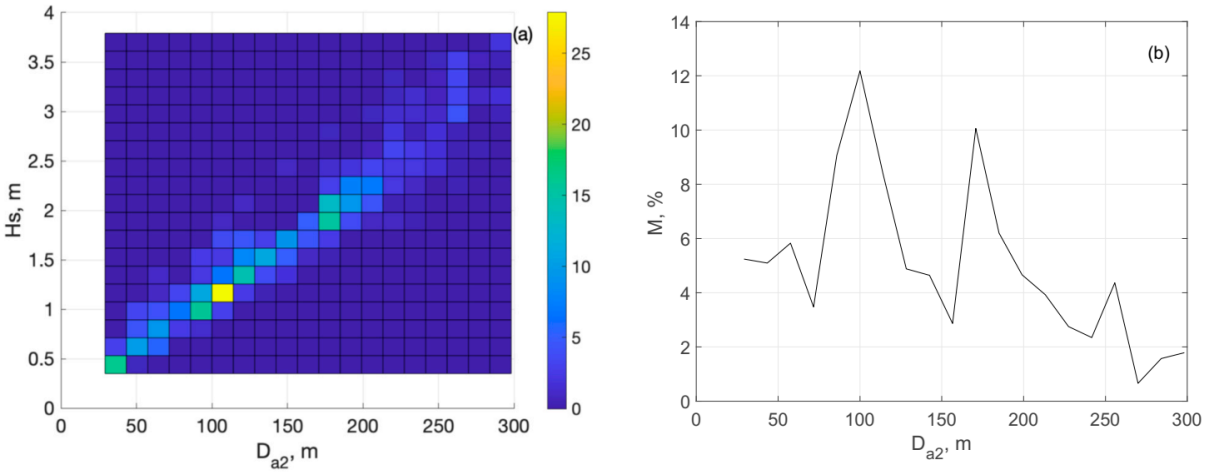

Figure 6. (**a**) Bivariate histogram depending on the value of the second harmonic maximum distance off the shoreline weighted by the dimensionless relation between the significant wave height and the depth of the second harmonic maximum; (**b**) wave impact metric (Equation (6)) in dependence on the distance from the second harmonic maximum to the shoreline.

4.2. Time Period 2: 9 November 2019–23 March 2020

During the previous period seaward, slope of the sand bar changed from 0.0185 to 0.0169. Decreasing of the bar slope leads to growth of percentage of the scenarios of wave transformation with periodic exchange of energy between harmonics (up to 71%) (Figure 7).

Percentage of wave regimes with shore-normal approach was only 26% during this period. As in the previous period, the highest waves approach the shore perpendicularly (Figure 7).

According to Figure 8, for the wave regimes that impact the underwater profile, second harmonic maximum is located 220 m (deep water wave steepness is in range [0.024, 0.027]) and 180 m off the coastline (deep water wave steepness is in the range [0.023, 0.03]), and the divergence point will be placed in the range between 150–220 m for the first case and 120–180 m in another. Field measurements show that during this period the bar crest moved 20–40 m shoreward to 170–190 m distance from the coastline (Figure 4, Table 1).

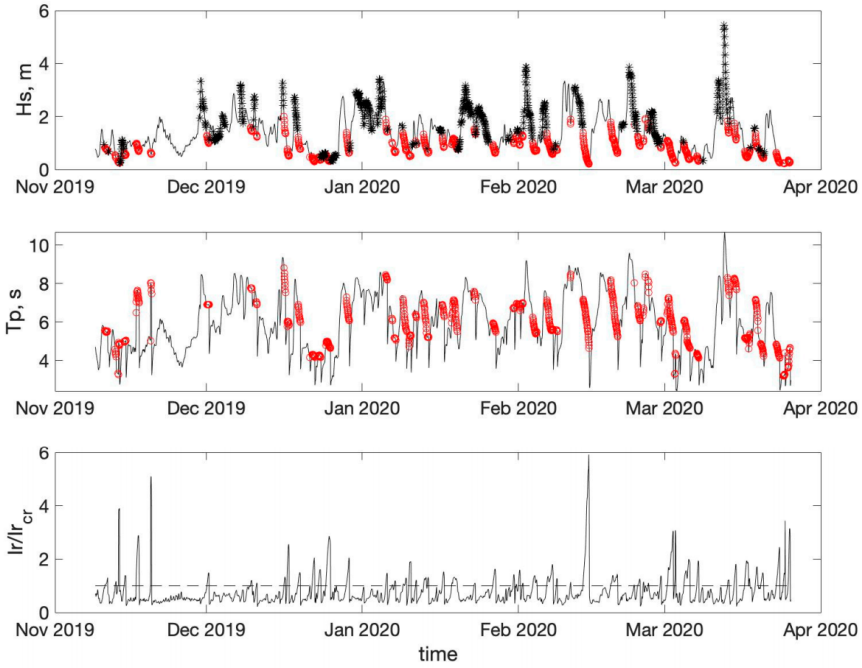

Figure 7. Wave height, peak wave period and ratio between deep water and critical Iribarren number (below the dashed line are regimes with pronounced exchange of energy between wave harmonics). Red circles—wave regimes without pronounced energy exchange between harmonics. Black stars—shore-normal regimes.

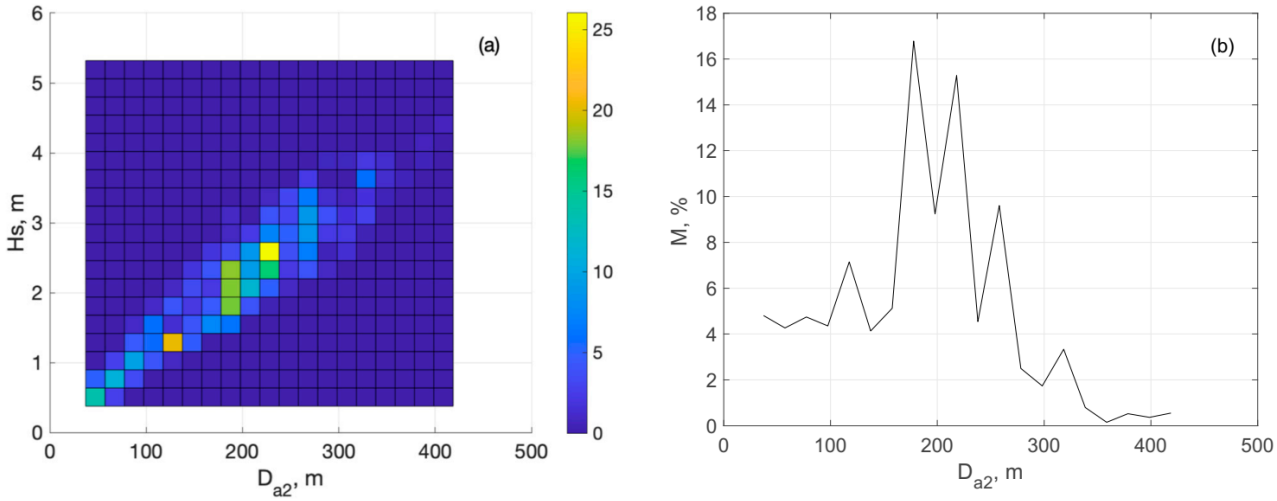

Figure 8. (**a**) Bivariate histogram depending on the value of the second harmonic maximum distance off the shoreline weighted by the dimensionless relation between the significant wave height and the depth of the second harmonic maximum; (**b**) wave impact metric (Equation (6)) dependent on the distance from the second harmonic maximum to the shoreline.

4.3. Time Period 3: 24 March–13 November 2020

With the progress of sand bar migration to the shore, the outer slope of the bar becomes milder and reaches 0.0161, but the percentage of the scenarios of wave transformation with periodic exchange of energy between harmonics stays nearly the same (72%), and 29% of all wave regimes are shore-normal (Figure 9).

With the decrease in bottom slope value, positions of the second harmonic maximum are scattered along the bottom slope with maxima at the 210, 160 and 120 distances off the shoreline (Figure 10), with ranges of the divergence point 140–210, 106–160 and 80–120.

Corresponding ranges of wave steepness are [0.02, 0.026], [0.02, 0.028] and [0.019, 0.026] respectively. The seaward slope of the sand bar becomes more uneven, at the same time the sand bar crest continues its onshore migration, and at the end of the considered period the sand bar crest was located 130–180 m off the coastline (Figure 4, Table 1).

The most repetitive wave regimes for this study site are characterized by deep water steepness about 0.023–0.024.

Thus, based on the estimates made, it can be concluded that the proposed method adequately describes the most probable position of the underwater bar for the periods under consideration. The position of the underwater bar corresponds to that observed on the studied site. The proposed simple method can be used to predict the underwater bar migration on the base of wave forecasting, hindcasting and reanalysis that can be important for coastal engineering projects and coastal management.

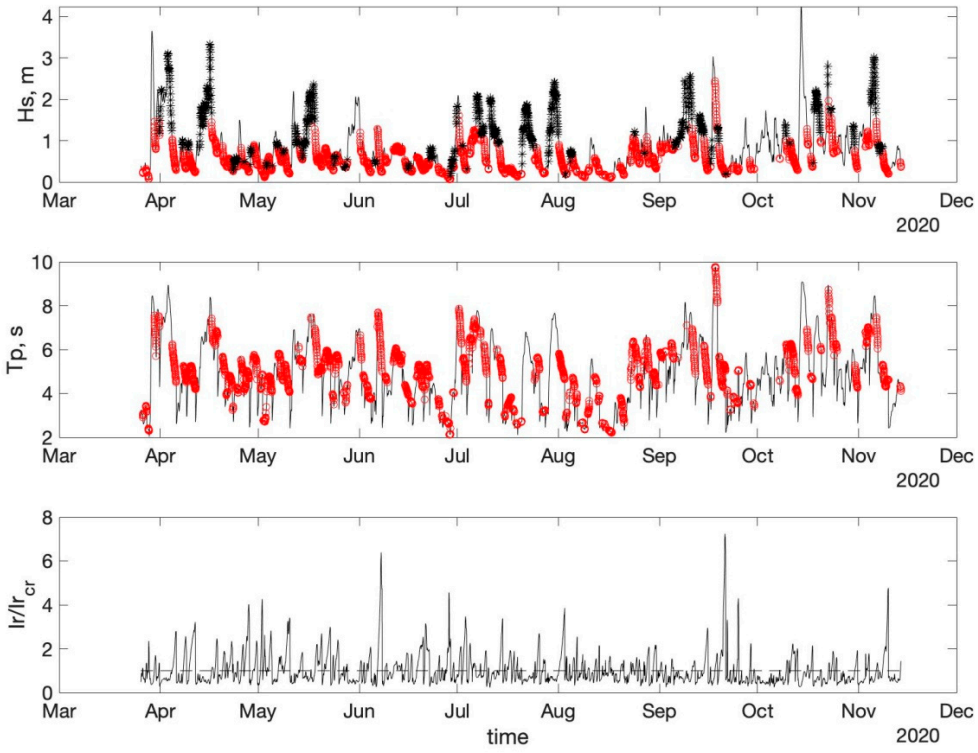

Figure 9. Wave height, peak wave period and ratio between deep water and critical Iribarren number (below the dashed line are regimes with pronounced exchange of energy between wave harmonics). Red circles—wave regimes without pronounced energy exchange between harmonics. Black stars—shore-normal regimes.

As was shown in [6], cross-shore sand bar migration is determined by storm duration and wave steepness.

The suggested method indirectly takes into account duration of storms automatically. The longer the storm lasts, the more points corresponding to the heights of the storm waves will be used in assessing the position of the bar.

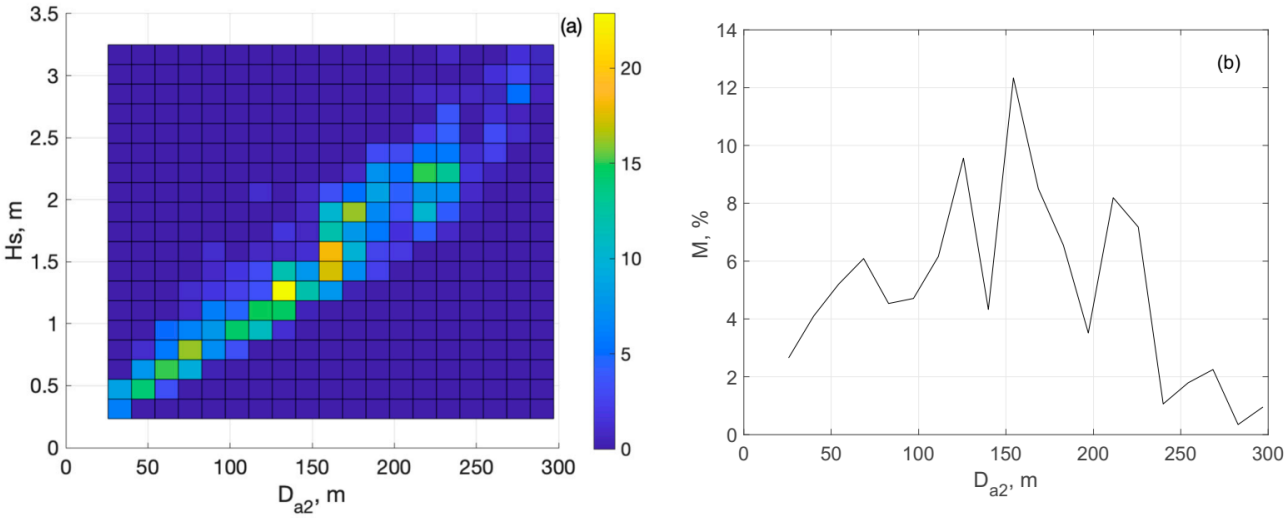

Figure 10. (**a**) Bivariate histogram depending on the value of the second harmonic maximum distance off the shoreline weighted by the dimensionless relation between the significant wave height and depth of the second harmonic maximum; (**b**) wave impact metric (Equation (6)) dependent on the distance from the second harmonic maximum to the shoreline.

Waves that cause sandbar migration are characterized by relatively high steepness to realize the necessary specific wave transformation scenario. For all the considered regimes deep water steepness exceeds 0.018.

Note that the scenario of wave transformations affecting bar formation and movement are defined by the relation between bottom slope and wave steepness through the Iribarren number (1–2). According to Equation (7):

$$\tan \alpha < 7\left(\frac{H}{L}\right)^{3/2} \quad (7)$$

So, if the bottom slope value is low, then waves with lower steepness are more responsible for bottom deformations. With an increase in the bottom slope the steepness of the waves that have influence the deformation of the relief will also increase. This can be seen from the experimental data analysis. In the most recurrent wave regimes that play a major role in the sandbar migration during the first time period, when the bottom slope is equal to 0.0185 wave steepness is in the range [0.026, 0.03]. However, when the bottom slope is of 0.0169 (second time period), the steepness of the most affecting waves is in the range [0.023, 0.03]. During the third time period when the bottom slope decreases to 0.0161, wave steepness is in the range [0.2, 0.28].

5. Conclusions

Mildly sloping sandy coasts' morpho-dynamics are strongly affected by wave transformation processes, one of which is a nonlinear triad interaction that leads to quasiperiodic changes in space of the wave profile due to periodic exchange of energy between 1 and 2 wave harmonics. This affects the formation and movement of the sand bars because second harmonic maximum position defines the divergence point for the sediment discharge. The prediction of the nearest shoreward position of the second harmonic maximum is the base of the methodology that allows location of the space range of the sand bars' formation positions. It was shown that steep waves cause sand bar migration, but critical wave steepness depends on bottom slope. Moreover, bottom slope, though mostly determined by geological properties of the region and by sediment balance, is also affected by sand bar migration. The changing bottom slope in the wave transformation region, caused by outer sand bar migration and evolution, also affects the processes of nonlinear wave transformation and changing of bar position. When the sand bar is formed by a strong

storm, the seaward slope of the bar becomes more than 30% steeper and the position of the second harmonic maximum and the point of sediment transport divergence moves onshore, followed by sand bar crest migration. This methodology does not concern the individual storm events: it is intended to assess the time series of wave regimes and their mutual influence on the sand bar migration. The wave climate is analyzed to distinguish the most significant wave regimes which are expected to define the sandbar motion and the range of its possible locations. The suggested method is simple, because it uses only arithmetical formulas, and allows hindcasting and forecasting of bar movements. Therefore, the proposed methodology can be useful for coastal zone management.

Author Contributions: Conceptualization, Y.S., M.S. and B.A.; methodology, Y.S. and M.S.; validation, M.S.; investigation, M.S.; writing—original draft preparation, M.S. and Y.S.; writing—review and editing, Y.S. and B.A. All authors have read and agreed to the published version of the manuscript.

Funding: This research was funded by Russian Foundation for Basic Research grant number 20-55-46005 and the Scientific and Technological Research Council of Turkey (TUBITAK) grant number 119N400.

Data Availability Statement: ERA5 reanalysis data is available here https://climate.copernicus.eu (access date 9 November 2021), Sentinel-2 satellite data is available here https://apps.sentinel-hub.com/eo-browser (access date: 9 November 2021), The bathymetry data is available upon request, please contact shtremel@ocean.ru.

Acknowledgments: This research was performed in the framework of the state assignment of Institute of oceanology of Russian Academy of Sciences, theme No. 0128-2021-0004.

Conflicts of Interest: The authors declare no conflict of interest.

References

1. Wright, L.D.; Short, A.D. Morphodynamic variability of surf zones and beaches: A synthesis. *Mar. Geol.* **1984**, *56*, 93–118. [CrossRef]
2. Lippmann, T.C.; Holman, R.A. The spatial and temporal variability of sand bar. *J. Geophys. Res.* **1990**, *95*, 11575–11590. [CrossRef]
3. Sallenger, A.H.; Holman, R.A.; Birkemeier, W.A. Storm induced response of a nearshorebar system. *Mar. Geol.* **1985**, *64*, 237–257. [CrossRef]
4. Gallagher, E.L.; Elgar, S.; Guza, R.T. Observations of sand bar evolution on a natural beach. *J. Geophys. Res.* **1998**, *103*, 3203–3215. [CrossRef]
5. Saprykina, Y. The Influence of Wave Nonlinearity on Cross-Shore Sediment Transport in Coastal Zone: Experimental Investigations. *Appl. Sci.* **2020**, *10*, 4087. [CrossRef]
6. Andreeva, N.; Saprykina, Y.; Valchev, N.; Eftimova, P.; Kuznetsov, S. Influence of Wave Climate on Intra and Inter-Annual Nearshore Bar Dynamics for a Sandy Beach. *Geosciences* **2021**, *11*, 206. [CrossRef]
7. Van Enckevort, I.M.J.; Ruessink, B.G. Video observations of nearshore bar behaviour. Part 1: Alongshore uniform variability. *Cont. Shelf Res.* **2003**, *23*, 501–512. [CrossRef]
8. Masselink, G.; Austin, M.; Scott, T.; Poate, T.; Russell, P. Role of wave forcing, storms and NAO in outer bar dynamics on a high-energy, macro-tidal beach. *Geomorphology* **2014**, *226*, 76–93. [CrossRef]
9. Ruessink, B.G.; Pape, L.; Turner, I.L. Daily to interannual cross-shore sandbar migration: Observations from a multiple sandbar system. *Cont. Shelf Res.* **2009**, *29*, 1663–1677. [CrossRef]
10. Nielsen, P. Selected unanswered challenges in coastal dynamics. In Proceedings of the Coastal Dynamics 2017, Helsingør, Denmark, 12–16 June 2017.
11. Kuznetsova, O.; Saprykina, Y. Influence of Underwater Bar Location on Cross-Shore Sediment Transport in the Coastal Zone. *J. Mar. Sci. Eng.* **2019**, *7*, 55. [CrossRef]
12. Plant, N.G.; Ruessink, B.G. On cross-shore migration and equilibrium states of nearshore sandbars. *J. Geophys. Res.* **2010**, *115*, F03008. [CrossRef]
13. Pape, L.; Ruessink, B.G.; Wiering, M.A.; Turner, I.L. Recurrent neural network modeling of nearshore sandbar behavior. *Neural Netw.* **2007**, *20*, 509–518. [CrossRef]
14. Roelvink, D.; Reniers, A.; van Dongeren, A.; van Thiel de Vries, J.; McCall, R.; Lescinski, J. Modelling storm impacts on beaches, dunes and barrier islands. *Coast. Eng.* **2009**, *56*, 1133–1152. [CrossRef]
15. Walstra, D.J.R.; Reniers, A.J.H.M.; Ranasinghe, R.; Roelvink, J.A.; Ruessink, B.G. On bar growth and decay during interannual net offshore migration. *Coast. Eng.* **2012**, *60*, 190–200. [CrossRef]
16. Roelvink, J.A.; Stive, M.J.F. Bar-generating cross-shore flow mechanisms on a beach. *J. Geophys. Res.* **1989**, *94*, 4785–4800. [CrossRef]

17. Kuriyama, Y. Process-based one-dimensional model for cyclic longshore bar evolution. *Coast. Eng.* **2012**, *62*, 48–61. [CrossRef]
18. Rafati, Y.; Hsu, T.J.; Elgar, S.; Raubenheimer, B.; Quataert, E.; van Dongeren, A. Modeling thehydrodynamicsandmorphodynamic-sofsandbarmigrationevents. *Coast. Eng.* **2021**, *166*, 103885. [CrossRef]
19. IFC Documentation—Cy46r1. Part VII: ECMWF Wave Model. European Centre for Medium-Range Weather Forecasts (ECMWF). Available online: https://www.ecmwf.int/en/elibrary/19311-ifs-documentation-cy46r1-part-vii-ecmwf-wave-model (accessed on 26 November 2021).
20. Shtremel, M. ERA5 wave data verification with buoy field measurements in the nearshore region of the Baltic Sea. In Proceedings of the 6th IAHR Europe Congress: No Frames No Borders, Warsaw, Poland, 15–18 February 2021; pp. 433–434. [CrossRef]
21. Boczar-Karakiewicz, B.; Davidson-Arnott, R. Nearshore bar formation by non-linear process—A comparison of model results and field data. *Mar. Geol.* **1987**, *77*, 287–304. [CrossRef]
22. Kuznetsov, S.; Saprykina, Y. Nonlinear Wave Transformation in Coastal Zone: Free and Bound Waves. *Fluids* **2021**, *6*, 347. [CrossRef]
23. Saprykina, Y.; Kuznetsov, S.Y.; Andreeva, N.; Shtremel, M. Scenarios of nonlinear wave transfor- mation in coastal zone. *Oceanology* **2013**, *53*, 422–431. [CrossRef]
24. Salem, A.S.; Jarno-Druaux, A.; Marin, F. Physical modeling of cross-shore beach morphodynamics under waves and tides. *J. Coast. Res.* **2011**, *64*, 139–143.
25. Saprykina, Y.V.; Shtremel, M.N.; Kuznetsov, S.Y. On the possibility of biphase parametrization for wave transformation in the coastal zone. *Oceanology* **2017**, *57*, 253–264. [CrossRef]